Title: Correlation between the 1:2 atomic order and microwave dielectric loss in the off-stoichiometric Ba($Zn_{1/3}Ta_{2/3}$)O_3

Author: Jintara Padchasri Rattikorn Yimnirun Taras Kolodiazhnyi

PII: S0955-2219(18)30174-2
DOI: https://doi.org/doi:10.1016/j.jeurceramsoc.2018.03.036
Reference: JECS 11793

To appear in: *Journal of the European Ceramic Society*

Received date: 9-3-2018
Revised date: 20-3-2018
Accepted date: 21-3-2018

Please cite this article as: Jintara Padchasri, Rattikorn Yimnirun, Taras Kolodiazhnyi, Correlation between the 1:2 atomic order and microwave dielectric loss in the off-stoichiometric Ba($Zn_{1/3}Ta_{2/3}$)O_3, *<![CDATA[Journal of the European Ceramic Society]]>* (2018), https://doi.org/10.1016/j.jeurceramsoc.2018.03.036

Correlation between the 1:2 atomic order and microwave dielectric loss in the off-stoichiometric $Ba(Zn_{1/3}Ta_{2/3})O_3$

Jintara Padchasri
School of Physics, Institute of Science and
NANOTEC-SUT COE on Advanced Functional Nanomaterials,
Suranaree University of Technology, Nakhon Ratchasima 30000, Thailand
Rattikorn Yimnirun
School of Energy Science and Engineering,
Vidyasirimedhi Institute of Science and Technology, Rayong 21210, Thailand
Taras Kolodiazhnyi*
National Institute for Materials Science, 1-1 Namiki, Tsukuba, Ibaraki, 305-0044, Japan

March 20, 2018

Abstract

We report close correlation between the 1:2 atomic order and microwave dielectric loss in the off-stoichiometric $Ba(Zn_{1/3}Ta_{2/3})O_3$ (BZT). Small off-stoichiometric deviations have a large effect on the ordering and $Q\times f$ values. The $Ba_4Ta_2O_9$-BZT-'$Zn_4Ta_2O_9$' pseudo tie line separating the Ta-rich and Ta-poor regions also demarcates the 1:2 ordered and disordered BZT. The low-loss off-stoichiometric BZT ceramics are located in the 1:2 ordered region of the BaO-ZnO-Ta_2O_5 phase diagram. Without exception the disordered BZT ceramics show high dielectric loss. Stoichiometric BZT with 1:2 atomic order shows $Q\times f = 113$ THz. The off-stoichiometric 1:2 ordered BZT ceramics with the highest $Q\times f >$ 200 THz are located in the ZnO-deficient part of the ternary phase diagram.

---

*Corresponding author; Tel.: +81-29-860-4407; Fax: +81-29-860-4706, E-mail: kolodiazhnyi.taras@nims.go.jp

1 Introduction

Since their conception in 1939 [1] followed by the first debut in late 60s of the last century [2], microwave dielectric resonators (DR) have become an intertwined part of the wireless communication industry. Among several families of DRs the $Ba(B'_{1/3}B''_{2/3})O_3$ perovskites with B′ = Zn, Mg, Co, and B″ = Nb and Ta show exceptionally good properties which secured their dominance in the up-link multiplexers for cell-phone base-stations. Despite some past attempts to replace the DRs with high-T_C superconductor filters and surface acoustic waveguides in the base stations, their widespread use will remain unchallenged in the foreseeable future.

More strict requirements are imposed on DRs to be used in the communication satellites: The DR must possess a dielectric constant, $20 \leq \varepsilon \leq 35$, temperature coefficient of the resonance frequency $+0.5 \leq \tau_f \leq +5$ ppm/K, $Q\times f$ product of ≥ 200 THz, where $Q = 1/\tan\delta$ and f is the resonant frequency. In addition, for geostationary satellites operating in the X-, Ku- and K-frequency bands, the DRs must have a stable τ_f in the range of −30 to +120 °C, and the unloaded $Q\times f \geq 130$ THz at $T = 120$°C. Because the $Q\times f$ drops with T, the latest requirement is very close to the intrinsic limit of the dielectric loss.[3] So far, only $Ba(Mg_{1/3}Ta_{2/3})O_3$ with $\varepsilon \approx 24$ and $Q\times f \approx 350$ THz at $T = 20$ °C can safely pass all the requirements.

Starting from the pioneering work of Fujimaru et al. [4], it was demonstrated that the small deviation from the ideal stoichiometry brings significant variation in the $Q\times f$ of $Ba(B'_{1/3}B''_{2/3})O_3$ perovskites [6, 7, 5]. In this contribution we find that the off-stoichiometric $Ba(Zn_{1/3}Ta_{2/3})O_3$ (hereafter abbreviated as BZT) shows $Q\times f \geq 200$ THz at $T = 20$ °C, which makes it potential DR candidate for X-band up-link satellite multiplexes because of its superior dielectric constant, $\varepsilon \approx 29$. We demonstrate that the high value of $Q\times f$ correlates closely with the 1:2 atomic order in $Ba(Zn_{1/3}Ta_{2/3})O_3$. Most remarkably, ceramics with $Q\times f > 200$ THz were found far away from the stoichiometric BZT composition which confronts our intuitive understanding of the sources of the extrinsic dielectric loss in $Ba(B'_{1/3}B''_{2/3})O_3$.

2 Experimental

DRs with 95 different off-stoichiometric compositions were prepared by conventional solid state ceramic technique. Precursor powders of Ta_2O_5, ZnO and $BaCO_3$ of 99.9% purity have been used. The precursor powders were thoroughly dried. The total weight of each batch was ∼ 15 g with a maximum weighing error less than 2 mg. This procedure has allowed to accurately control the off-stoichiometry of the target compositions. The powder mixtures were milled for 20 h in plastic bottles with ethanol and zirconia grinding balls. After calcination at 1200°C for 5 h the milling was repeated, the slurry dried and mixed with PVA binder, screened through the 120 mesh nylon sieve and uniaxially pressed into green pucks of ca. 7 mm diameter and 3 mm thickness. The pucks were muffled in yttrium oxide and sintered at 1550 °C for 10

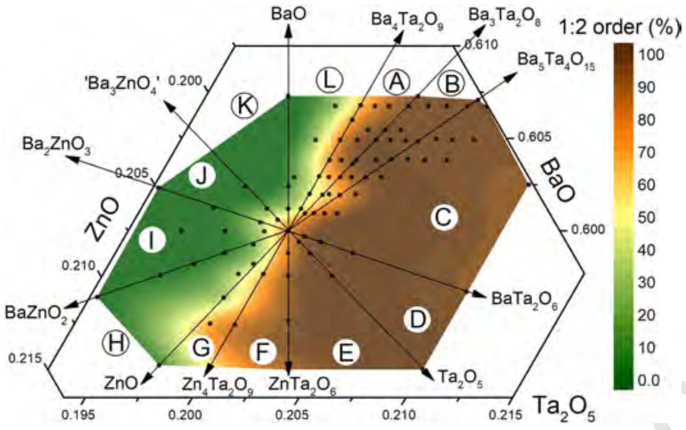

Figure 1: 1:2 B-site cation order in the vicinity of the BZT for ceramics sintered at 1550°C and annealed at 1450°C. The axis numbers are the mole fractions of the corresponding oxides labeled in large font. Large letters *A*-*L* indicate the composition sectors. The data are adapted from Ref. [8] with permission from Elsevier.

h followed by anneal at 1450°C for 20 h. The unloaded Q-factor, ε and τ_f were measured at 10–11 GHz in transmission mode (s_{21} parameter) using cylindrical cavity connected to the ports of the HP8719 vector network analyzer. To make certain that the first resonance is of the $TE_{01\delta}$-type, the DR pucks were prepared with diameter to thickness ratio of $\approx 2.26\pm0.03$. The description of the microwave (MW) measurements are given in Ref. [5]. The unloaded Q-factor was calculated according to:

$$Q = \frac{Q_L}{1 - 10^{-P/20}} \tag{1}$$

where Q_L is the loaded quality factor determined from the full width of the resonance peak at the 3 dB level, and P is the absolute value of the s_{21} parameter at the resonance in dB. The scatter of the Q-factor of DR pucks of the same composition did not exceed 5 %. To minimize the coupling, the s_{21} parameter at the resonance peak was adjusted to around -30 dB. Temperature coefficient of the resonance frequency, τ_f, was measured in the temperature interval of +20 to +70 °C and obtained according to:

$$\tau_f = \frac{\Delta f}{f_0 \times \Delta T}, \tag{2}$$

where Δf is a shift of the resonant frequency, f_0, introduced by a temperature change of ΔT.

3 Results and discussion

The details of the effect of the off-stoichiometry on the phase composition, microstructure, lattice distortion and the 1:2 cation order in BZT have been reported in Ref. [8]. Fig. 1 shows an effect of the deviation from the stoichiometry on the degree of the long-range 1:2 B-site order in BZT. To streamline the discussion, the

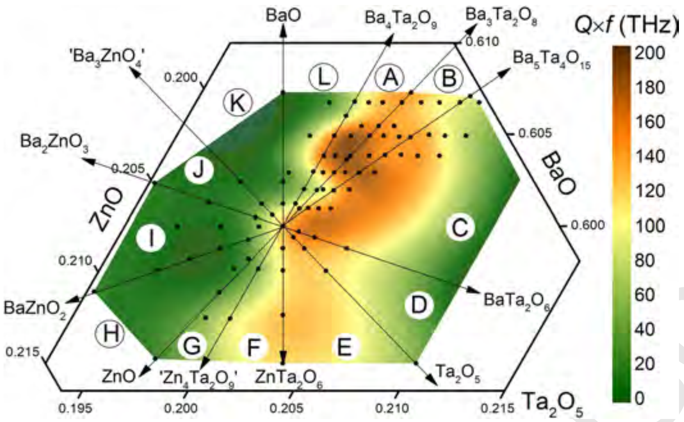

Figure 2: $Q\times f$ values of the off-stoichiometric BZT ceramics sintered at 1550°C for 10 h and annealing at 1450°C for 20 h. The black dots indicate the target composition. The axis numbers are the mole fractions of the corresponding oxides labeled in large font. Large letters A-L indicate the composition sectors.

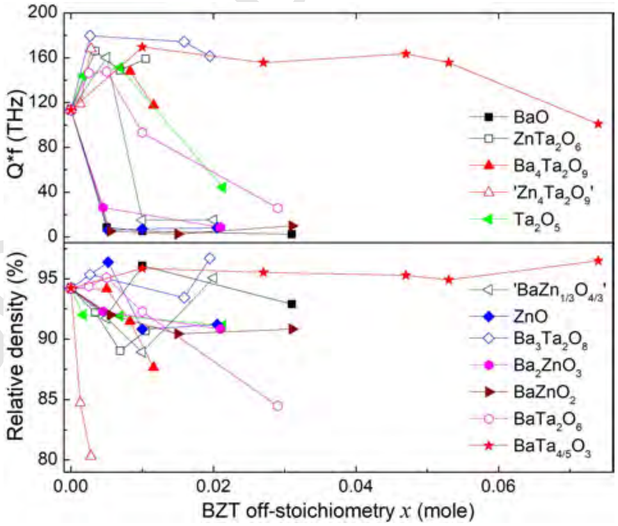

Figure 3: Summary of the $Q\times f$ values (top panel) and ceramic density (bottom panel) along the selected (pseudo) tie lines originating from the stoichiometric BZT.

BaO-ZnO-Ta_2O_5 phase map is divided into the sectors $A, B, C...L$. However, the phase map introduced here is intended for discussion purposes only and should not be confused with a true equilibrium phase diagram of the pseudo-ternary BaO-ZnO-Ta_2O_5 system [9]. Both ordered ($P\bar{3}m1$ space group) and disordered ($Pm3m$ space group) BZT ceramics were obtained in this study. A closer look at Fig. 1 reveals a boundary separating the ordered and disordered BZT that runs approximately along the '$Zn_4Ta_2O_9$'-BZT-$Ba_4Ta_2O_9$ pseudo tie line.

According to earlier reports [6], BZT is not a point compound but accommodates some finite concentration of the point defects upon deviation from stoichiometry. As such, the point defect chemistry is probably a key to understanding the order-disorder BZT map in Fig. 1. Ignoring Frenkel disorder and binary Schottky defects and assuming that the Schottky defects are fully ionized, the point defect equilibrium involving Schottky and anti-site defects, according to the Kröger-Vink notation, is given by:

$$\begin{aligned} 2[V''_{\mathrm{Ba}}] + 2[V''_{\mathrm{Zn}}] + 5[V'''''_{\mathrm{Ta}}] + 3[\mathrm{Zn}'''_{\mathrm{Ta}}] + 3[\mathrm{Ba}'''_{\mathrm{Ta}}] + [\mathrm{Zn}^{\times}_{\mathrm{Ba}}] + \\ + [\mathrm{Ba}^{\times}_{\mathrm{Zn}}] = 2[V^{\bullet\bullet}_{\mathrm{O}}] + 3[\mathrm{Ta}^{\bullet\bullet\bullet}_{\mathrm{Zn}}] + 3[\mathrm{Ta}^{\bullet\bullet\bullet}_{\mathrm{Ba}}] \end{aligned} \quad (3)$$

According to literature, electrostatic interaction between the B-site ions is the main driving force of the 1:2 B-site cation ordering [10]. Therefore, a disruption of the periodic electrostatic potential with the highly charged point defect will frustrate the 1:2 order. Among the point defects listed in Eq. 3, the V'''''_{Ta} defect has the highest electrostatic charge which will bring the strongest random field potential in the BZT lattice. Because the sectors $A-F$ are located in the Ta_2O_5-rich part of the BaO-ZnO-Ta_2O_5 phase diagram, the chemical potential of Ta ion in the BZT compound at the single phase boundary with the $Ba_4Ta_2O_9$, $Ba_3Ta_2O_8$ and $Ba_5Ta_4O_{15}$ phases is high and the formation of the V'''''_{Ta} defects will be suppressed [11]. In contrast, the chemical potential of Ta in BZT facing the secondary phases in the $G-L$ sectors is low leading to higher concentration of the V'''''_{Ta} defects. It is therefore very tempting to attribute the 1:2 B-site atomic order in the off-stoichiometric BZT to the thermodynamics of the V'''''_{Ta} point defect.

Figure 2 shows the effect of stoichiometry on the $Q{\times}f$ of the BZT ceramics, whereas Table 1 reports the $Q{\times}f$, ε and τ_f data for selected off-stoichiometric BZT. There are some striking similarities between the 1:2 order and the $Q{\times}f$ maps of the off-stoichiometric BZT. Without exception, it appears that the high $Q{\times}f$ values are found in the BZT ceramics with the high degree of the 1:2 atomic order, i.e., in ceramics located in the sectors $A-F$ (see Figs. 1 and 2). None of the disordered ceramics in the sectors $H-L$ shows a high $Q{\times}f$ value. The boundary between the high- and low-Q ceramics lies approximately along the '$Zn_4Ta_2O_9$'-BZT-$Ba_4Ta_2O_9$ pseudo tie line, similar to the boundary separating the 1:2 ordered and disordered BZT (Fig. 1). Therefore, in agreement with earlier reports [12, 13, 6] we confirm that the 1:2 order is a necessary requirement for the high-Q BZT ceramics.

Another important finding is that the highest $Q{\times}f$ ceramics with $Q{\times}f > 200$ THz are found in sectors A, B and C (Fig. 2 and Table 1) far away from the stoichiometric BZT with $Q{\times}f \approx 113$ THz. For example,

Table 1: Target chemical composition (mole) rounded to 4 decimal places, ε, $Q\times f$ and τ_f of selected BZT ceramics. The samples' letter indicates the composition sector specified in Fig. 1, while two letters indicate that the sample is located on the boundary between the two sectors. Asterisk indicates disordered perovskites.

sample	BaO	ZnO	Ta_2O_5	ε	$Q\times f$ (THz)	τ_f (ppm/K)
1	0.6000	0.2000	0.2000	28.0	113	–1.9
KL4*	0.6073	0.1963	0.1964	28.6	2	–19.7
EF6	0.5976	0.2012	0.2012	27.1	149	–2.0
AB14	0.6055	0.1927	0.2018	28.4	174	–0.8
CD31	0.5994	0.1988	0.2018	28.6	147	–1.3
CD32	0.5988	0.1976	0.2036	28.1	105	+2.2
HI34*	0.5976	0.2072	0.1952	28.1	4	–1.0
BC39	0.6029	0.1949	0.2022	27.9	167	–2.0
IJ50*	0.6013	0.2028	0.1959	28.2	5	–2.2
A61	0.6049	0.1943	0.2008	26.8	204	–1.8
EF86	0.5925	0.2038	0.2037	26.5	115	–1.0
L97*	0.6067	0.1944	0.1988	28.5	4	–17.5

sample A61 (see Table1) shows $Q\times f$ = 204 THz which is comparable with the $Q\times f$ =141 THz estimated from the far infrared reflectance of the BZT ceramics.[15] Furthermore, the highest-Q BZT are not single-phase but contain a very small amounts of the second phases, predominantly $Ba_8ZnTa_6O_{24}$. Apparently, the 8-layer hexagonal perovskite $Ba_8ZnTa_6O_{24}$ does not cause significant reduction of the Q-factor [14]. In contrast, the $Ba_9ZnTa_{14}O_{45}$ phase with tetragonal tungsten bronze (TTB) structure causes significant decrease in the Q-factor upon deviation from the BZT-$Ba_5Ta_4O_{15}$ tie line into the C sector. Similar trend has been detected in the off-stoichiometric $Ba(Mg_{1/3}Ta_{2/3})O_3$ ceramics [5].

In addition to the BZT, several other $Ba(B'_{1/3}B''_{2/3})O_3$ perovskites show a significant increase in the Q-factor in the $B'O$-deficient part of the phase diagram, i.e., in the A and B sectors and in the part of the sector C neighbouring the $Ba(B'_{1/3}B''_{2/3})O_3$-$Ba_5B''_4O_{15}$ tie line [7, 16, 17, 5, 18]. To explain the enhancement of the Q-factor in the off-stoichiometric $Ba(B'_{1/3}B''_{2/3})O_3$ several models have been proposed. Among them an improvement in the microstructure and density [19], coarsening of the 1:2 ordered domains and subsequent elimination of the anti-phase domain boundaries [20], point defect engineering [7, 5], trigonal lattice distortion [12], microwave absorption by paramagnetic impurities [21], etc.

According to the data in Figure 3, high density is probably important but it is not sufficient to guarantee the high $Q\times f$. Indeed ceramics along the BZT-$Ba_4Ta_4O_{15}$ and BZT-$Ba_3Ta_2O_8$ tie lines show both high density and high $Q\times f$. In contrast, ceramics formulated along the BZT-ZnO tie line show low $Q\times f$ but relatively high density of ≈ 91-96 % whereas ceramics with target composition along the BZT-'$Zn_4Ta_2O_9$' pseudo tie line show high $Q\times f$ but rather low density of ≈ 81-85 %.

Table 1 also summarizes the effect of the off-stoichiometry on the τ_f. The stoichiometric BZT (i.e., sample 1) shows $\tau_f = -1.9$ ppm/K. The τ_f of the high-Q off-stoichiometric BZT located in the A, B and C sectors (i.e., samples AB14, BC39, A61) fluctuates in the narrow range of -1.4 ± 0.6 ppm/K. The low-Q disordered BZT located close to the BZT-BaO tie line (i.e., samples KL4* and L97*) show large negative $\tau_f \approx -19$ ppm/K probably due to the effect of the $Ba_4Ta_2O_9$ or BaO secondary phases. The τ_f of ceramics along the BZT - $BaTa_2O_6$ tie line (samples CD31 and CD32 in Table1) changes sign from negative to positive as a result of the TTB second phase, similar to the case reported in the off-stoichiometric $Ba(Mg_{1/3}Ta_{2/3})O_3$ [5].

Desu and O'Bryan explained an increase in the Q-factor of BZT during the prolonged high-temperature anneal by the loss of Zn [12]. The loss of Zn effectively shifts the ceramic composition from the stoichiometric BZT along the BZT-$Ba_3Ta_2O_8$ tie line. The subsequent increase in the trigonal lattice distortion was attributed by the authors to the formation of the anti-site $Ba_{Zn}^{\times}$ defect [12]. This original hypothesis was extended to the $Ba(Mg_{1/3}Ta_{2/3})O_3$ system that also show significant improvement of $Q\times f$ in the neighbourhood of the $Ba(Mg_{1/3}Ta_{2/3})O_3$-$Ba_3Ta_2O_8$ tie line [5]. Furthermore, a low-temperature dielectric relaxation in the MgO-rich $Ba(Mg_{1/3}Ta_{2/3})O_3$ with low Q-factor was taken as an evidence of the Mg 'rattling' in the anti-site $Mg_{Ba}^{\times}$ defect [5]. However, in addition to the anti-site defects, the high and low chemical potential of Zn in BZT can be also accommodated by the $[V_{\mathrm{Ba}}''\text{-}V_{\mathrm{O}}^{\bullet\bullet}]$ and $[V_{\mathrm{Zn}}''\text{-}V_{\mathrm{O}}^{\bullet\bullet}]$ Schottky defects, respectively. It is obvious that the first-principles calculations of the defect equilibrium and its effect on the 1:2 order and dielectric loss in BZT and other $\mathrm{Ba(B'_{1/3}B''_{2/3})O_3}$ perovskites are necessary to perfect the DR properties.

4 Conclusion

In conclusion, it is demonstrated that the slight deviation from the stoichiometric BZT brings about dramatic changes in the long-range 1:2 B-site cation order and microwave dielectric loss. The boundary separating the 1:2 ordered and disordered BZT lies approximately along the '$\mathrm{Zn_4Ta_2O_9}$'-BZT-$\mathrm{Ba_4Ta_2O_9}$ pseudo tie line. The same boundary also separates the Ta-rich and Ta-poor off-stoichiometric BZT compositions. Our attempts to find a high-Q BZT in the region of the disordered compositions were unsuccessful: All disordered off-stoichiometric BZT ceramics studied here show very low $Q{\times}f$ value. This finding confirms once again that the 1:2 B-site cation order is a necessary condition for the low-loss BZT ceramics. A two-fold improvement of the $Q{\times}f$ from 113 THz to 204 THz was found upon deviation from the stoichiometric BZT to the ZnO-deficient BZT thus making it a potential DR candidate for the up-link satellite multiplexers.

T.K. thanks R&D staff of Com Dev Int. for their interest in this work. J.P. work at NIMS was supported by the Science Achievement Scholarship of Thailand (SAST) and internal NIMS grant PA402.

References

[1] Richtmyer RD. Dielectric resonators. *J. Appl. Phys.* 1939;**10**:391–8.

[2] Cohn SB. Microwave bandpass filters containing high-Q dielectric resonators. *IEEE Trans. Microwave Theory Tech.* 1968;**16**:218–27.

[3] Kolodiazhnyi T, Annino G, Shimada T. Intrinsic limit of dielectric loss in several $\mathrm{Ba(B'_{1/3}B''_{2/3})O_3}$ ceramics revealed by the whispering-gallery mode technique. *Appl. Phys. Lett.* 2005;**87**:212908.

[4] Fujimaru T, Nishida M, Kugimiya K. US Patent 5246898.

[5] Kolodiazhnyi T. Origin of extrinsic dielectric loss in 1:2 ordered, single-phase $\mathrm{Ba(Mg_{1/3}Ta_{2/3})O_3}$. *J. Eur. Ceram. Soc.* 2014;**34**:1741–53 .

[6] Koga E, Yamagishi Y, Moriwake H, Kakimoto K, Ohsato H. Large Q factor variation within dense, highly ordered $\mathrm{Ba(Zn_{1/3}Ta_{2/3})O_3}$ system. *J. Eur. Ceram. Soc.* 2006;**26**:1961–4.

[7] Wu H, Davies PK. Influence of non-stoichiometry on the structure and properties of $\mathrm{BaZn_{1/3}Nb_{2/3}O_3}$ microwave dielectrics: II. Compositional variations in pure BZN. *J. Am. Ceram. Soc.* 2006;**89**:2250–63.

[8] Kolodiazhnyi T, Padchasri J, Yimnirun R. Effect of temperature and stoichiometry on the long-range 1:2 cation order in $Ba(Zn_{1/3}Ta_{2/3})O_3$. *J. Eur. Ceram. Soc.* 2018;**38**: 1517–23.

[9] Vanderah TA, Pickett E, Levin I, Roth RS. Ternary subsolidus for the system BaO-ZnO-Ta_2O_5. NIST Phase Equilibria Diagrams Fig. 11283.

[10] Bellaiche L, Padilla J, Vanderbilt D. Heterovalent and A-atom effects in $A(B'B'')O_3$ perovskite alloys. *Phys Rev B* 1999;**59**:1834–9.

[11] Schmalzried H, *Solid State Reactions* (Verlag Chemie, Weinheim, 1981) p.7.

[12] Desu SB, O'Bryan HM. Microwave loss quality of $Ba(Zn_{1/3}Ta_{2/3})O_3$ ceramics. *J. Am. Ceram. Soc.* 1985;**68**:546–51.

[13] Kawashima S, Nishida M, Ueda I, Ouchi H. $Ba(Zn_{1/3}Ta_{2/3})O_3$ ceramics with low dielectric loss at microwave frequencies. *J. Am. Ceram. Soc.* 1983;**66**:421–3.

[14] Moussa SM, Claridge JB, Rosseinsky MJ, Clarke S, Ibberson RM, Price T, Iddles DM, Sinclair DC. $Ba_8ZnTa_6O_{24}$: a high-Q microwave dielectric from a potentially diverse homologous series. *Appl. Phys. Lett.* 2003;**82**:4537–39.

[15] Tamura H, Sagala DA, Wakino K. Lattice vibrations of $Ba(Zn_{1/3}Ta_{2/3})O_3$ crystal with ordered perovskite structure. *Jpn. J. Appl. Phys.* 1986;**25**:787–791.

[16] Paik JH, Nahm S, Bylin JD, Kim MH, Lee HJ. The effect of Mg defciency on the microwave dielectric properties of $BaMg_{1/3}Nb_{2/3}O_3$ ceramics. *J. Mat. Sci. Lett.* 1998;**17**:1777–80.

[17] Belous AG, Ovchar OV, Kramarenko AV, Jancar B, Bezjak J, Suvorov D, Effect of Nontoichiometry on the Structure and Microwave Dielectric Properties of $BaCo_{1/3}Nb_{2/3}O_3$. *Inorg. Mat.* 2010;**46**:529–33.

[18] Sayyadi-Shahraki A, Taheri-Nassaj E, Gonzales J, Newman N, Kolodiazhnyi T. Effect of non-stoichiometry on the densification, phase purity, microstructure, crystal structure, and dielectric loss of $BaCo_{1/3}Nb_{2/3}O_3$ ceramics. *J. Eur. Ceram. Soc.* 2017;**37**:3335-46.

[19] Koga E, Mori H, Kakimoto K, Ohsato H. Synthesis of disordered $Ba(Zn_{1/3}Ta_{2/3})O_3$ by spark plasma sintering and its microwave Q factor. *Jpn. J. Appl. Phys.* 2006;**45**:7484–88.

[20] Davies PK, Tong J, Negas T, Effect of orderinginduced domain boundaries on lowloss $Ba(Zn_{1/3}Ta_{2/3})O_3BaZrO_3$ perovskite microwave dielectrics. *J. Am. Ceram. Soc.* 1997;**80**:1727-40.

[21] Liu L, Flores M, Newman N, Microwave loss in the high-performance dielectric $Ba(Zn_{1/3}Ta_{2/3})O_3$ at 4.2 K. *Phys. Rev. Lett.* 2012;**109**:257601.